Skin microbial dysbiosis is a characteristic of systemic drug-related intertriginous and flexural exanthema-like lesions induced by EGFR inhibitor

Wenqi Liu [a], Lu Peng [a], Ling Chen [b], Jianji Wan [a], Shuang Lou [a], Tingting Yang [a], Zhu Shen [a,*]

[a] *Department of Dermatology, Guangdong Provincial People's Hospital (Guangdong Academy of Medical Sciences), Southern Medical University, Guangzhou, 510080, China*
[b] *Department of Dermatology, Daping Hospital, Army Medical University, Chongqing, 400042, China*

ARTICLE INFO

ABSTRACT

Objectives: To investigate the characteristics of the skin microbiome in severe afatinib-induced skin toxicity.
Methods: Body site-matched skin surface samples were collected from the lesions on seven flexural sites of one lung cancer (Patient 1) with serious systemic drug-related intertriginous and flexural exanthema (SDRIFE)-like toxicity induced by EGFR-TKI and three healthy age/sex matched controls for whole metagenomics sequencing analysis. Lung cancer Patient 1 and Patient 2 were prescribed minocycline and followed up.
Results: In SDRIFE-like toxicities induced by afatinib, lesion microbiota richness (ACE and Chao1 index: $p < 0.001$) and diversity (Shannon's and Simpson's diversity indices: $p < 0.01$) were reduced. Similarly, the beta diversity analysis ($R = 1$, $p = 0.002$ for ANOSIM) showed that the apparent difference in the microbiota composition was statistically significant. The microbial taxa composition in the patient showed an increased abundance of pathogenic bacteria and a decreased abundance of commensal bacteria. LEfSe analysis identified strong bacterial pathogenicity in the patient, while healthy controls exhibited enrichment in several pathways that are beneficial for skin commensal bacteria and skin physiology, including key amino acid metabolism, energy/lipid/glycan biosynthesis/metabolism, and cofactors/vitamins biosynthesis. Ultimately, the patients experienced significant improvement with minocycline.
Conclusion: Microbial dysbiosis is a characteristic of severe SDRIFE-like toxicity induced by afatinib.

1. Introduction

Small molecule inhibitors, including epidermal growth factor receptor-tyrosine kinase inhibitors (EGFR-TKIs), have become the current trend in oncology treatment [1]. EGFR is expressed in the basal layer of the epidermis where its roles include stimulation of epidermal growth and inhibition of its differentiation. EGFR is one of the most commonly mutated oncogenes, and this central role

makes it an important therapeutic target in tumors that depend on the EGFR pathways [2]. At the same time, EGFR-TKIs can lead to related adverse events (AEs), including serious dermatological ones [3–5]. Afatinib, as a second-generation EGFR-TKI, inhibits wild-type EGFR more effectively, resulting in higher rate of skin and gastrointestinal toxicity [1]. The incidences of skin reactions are 90 % [5], but the pathogenesis of EGFR-TKI-induced skin toxicity remains incompletely understood.

On the skin, many microbial species successfully colonize, known as the commensal microbiome, to protect against pathogen invasion and ensure skin homeostasis. A broken barrier is a potent trigger for skin inflammation. The interplay among the epithelial barrier, immune inflammation, and the cutaneous microbiome has been considered vital for maintaining a balance between health and disease [6]. Considering the effects of EGFR-TKI on epidermal cell differentiation and barrier function, the skin toxicity induced by EGFR-TKI does not exclude the involvement of an imbalance in the skin flora.

In this study, we aim to verify that skin microbial dysbiosis is a characteristic of severe systemic drug-related intertriginous and flexural exanthema (SDRIFE)-like skin toxicities induced by EGFR inhibitors. To achieve this, we performed metagenomic sequencing in SDRIFE-like skin toxicities induced by afatinib. SDRIFE is a cutaneous AE that presents a characteristic eruption with following systemic absorption of medication. There are five proposed criteria for SDRIFE features and it is an increasingly recognized AE of EGFR inhibitors [7]. Based on a report summarizing the characteristics of prior cases secondary to EGFR inhibition, we found that the patient treated with minocycline exhibited faster remission and lower recurrence rates of SDRIFE compared to those treated solely with topical glucocorticoids [8].

According to the experimental results, we demonstrated that the diversity/richness of the lesional microbiota decreased, and its microbial composition changed: there was an increased abundance of pathogenic bacteria and a decrease in commensal bacteria. Moreover, the patient group had strong pathogenicity (e.g., biofilm formation). Meanwhile, LEfSe analysis of functional differences prediction in the control group revealed a high enrichment of pathways beneficial to skin commensal bacteria and skin physiology. These pathways include key amino acid metabolism (e.g., tryptophan biosynthesis), energy/lipid metabolism models, cofactors/vitamins biosynthesis, and glycan biosynthesis. Lastly, the patient experienced significant long-term improvement of her SDRIFE-like lesions with minocycline treatment while continuing regular use of afatinib.

Our investigation supports the critical role of microbial dysbiosis involved in serious SDRIFE-like toxicity induced by afatinib. It also provides evidence for the use of antibiotics during the treatment of EGFR-TKIs, which can enhance patient quality of life and improve adherence to anti-cancer therapy.

2. Methods

2.1. Study participants

Patient 1 and Patient 2 were diagnosed as adverse drug reaction of EGFR-TKIs at Guangdong Provincial People's Hospital, Guangzhou, China. Three healthy age- and sex-matched controls were recruited, and they had no active infection, antibiotic or probiotic use in the previous 4 weeks. Subjects were instructed to refrain from using topical products for two days before sampling. The study was approved by the Ethics Committee of Guangdong People's Hospital (Approval No: KY-N-022-109-01). All subjects provided written informed consent.

2.2. Sample collection

Single time-point sample collection was performed on seven flexural sites (Supplementary Fig. 1). Each skin sample was collected by swabbing with sterile DNA-free cotton swabs. The swabbing area covered approximately the same area as a circle with a radius of 2 cm [9]. The cotton tips were cut, placed into sterile containers, and immediately frozen in liquid nitrogen for 5 min before being transferred to −80 °C for storage until DNA extraction [10].

2.3. DNA extraction and library construction

Total genomic DNA was extracted from the clipped swabs using a MagPure Soil DNA KF Kit (MP, Guangzhou, China) following the manufacturer's instructions. The concentration and integrity of the DNA were assessed using a NanoDrop2000 spectrophotometer (Thermo Fisher Scientific, Waltham, MA, USA) and agarose gel electrophoresis, respectively. The DNA was fragmented using S220 Focused-ultrasonicators (Covaris, USA) and purified with Agencourt AMPure XP beads (Beckman Coulter Co., USA). Subsequently, libraries were constructed using the TruSeq Nano DNA LT Sample Preparation Kit (Illumina, San Diego, CA, USA) according to the manufacturer's instructions. The specific primer sequences used for library construction are as follows:
VAHTS Adapter-S for Illumina:
5′-ACACTCTTTCCCTACACGACGCTCTTCCGATC-*s*-T-3′
3′-CTGACCTCAAGTCTGCACACGAGAAGGCTAG-p-5′
VAHTS i5 PCR Primers:
5′-AATGATACGGCGACCACCGAGATCTACAC[i5]ACACTCTTTCCCTACACGACGCTCTTCCGATC-*s*-T-3′
VAHTS i7 PCR Primers:
5′-CAAGCAGAAGACGGCATACGAGAT[i7]GTGACTGGAGTTCAGACGTGTGCTCTTCCGATC-*s*-T-3′
(-*s*: Phosphorthioate, -p: phosphorylation)

2.4. Metagenomic sequencing and bioinformatic analysis

Metagenomic sequencing was conducted using the Illumina NovaSeq6000 high-throughput sequencing platform at OE Biotech (Shanghai, China), following its standard procedures and published literature [11,12]. Paired-end sequencing with a read length of 150 bp was performed on the Illumina NovaSeq6000 platform. Quality control of the raw metagenomic sequencing data was conducted using the fastp software (https://github.com/OpenGene/fastp) [13]. The sequences in FASTQ format were trimmed and filtered using Trimmomatic (v 0.36). Host pollution control was set.The post-filtered pair-end reads were aligned against the host genome using Bowtie2 (v 2.2.9), and the aligned reads were discarded. After obtaining valid reads through quality control, metagenome assembly was performed using MEGAHIT (v 1.1.2). Gaps inside the scaffold were utilized as breakpoint to interrupt the scaffold into new contigs (Scaftig), and these new Scaftigs with length >500 bp were retained for statistics and used for subsequent analysis. Open reading frames (ORFs) prediction of assembled scaffolds was carried out using Prodiga (v 2.6.3), and these ORFs were translated into amino acid sequences. Then, all predicted genes were clustered using CD-HIT (V 4.6.7), with parameters set at 95 % identity and 90 % coverage, to generate non-redundant gene sets. The longest gene was chosen as representative sequence of each gene set. Clean reads of each sample were aligned against the non-redundant gene set (95 % identity) with Bowtie2 (v 2.2.9), and the abundant information of the gene in the corresponding sample was counted. Taxonomic annotation was conducted by aligning the non-redundant gene catalog against the NCBI-NR database using the basic local alignment search tool for proteins (BLASTP), with an e-value cutoff of 1e-5. DIAMOND (v 0.9.7) software was employed to compare the representative sequences in the non-redundant gene set with the NR Library of NCBI, and annotations with e < 1e-5 were taken. The taxonomy of the species was obtained based on the corresponding taxonomy database of the NR Library, and the abundance of the species was calculated using the corresponding abundance of the genes.

2.5. Statistical analysis of microbial compositions and functions

Differential abundance analyses were conducted at both species and genus levels for the seven body sites. The differential expression of bacterial genes was identified by comparing relative abundances. Wilcoxon's rank-sum test was analyzed to evaluate the differences in the relative abundance of microbial communities. Bacterial richness and diversity among samples were assessed using α indexes (ACE, Chao1, Shannon, and Simpson). Based on the relative abundances, the student's *t*-test was employed to compare the α diversity indices. Principal coordinates analysis (PCoA) and hierarchical clustering was applied to compare the bacterial composition between samples using Bray Curtis distance. Additionally, an analysis of similarities (ANOSIM) was performed to evaluate the significance of differences in community structure between the two groups using β diversity indices. Spearman correlations were utilized to calculate the relationships among the dominant microbial species. Linear discriminant analysis coupled with effect size (LEfSe) measurement was performed to determine the significant pathways of Kyoto Encyclopedia of Genes and Genomes (KEGG) between the two groups. The results were visualized using bar charts [14]. Linear discriminant analysis (LDA) values > 3.0 with a P-value < 0.05 were considered as significantly enriched. Virulence factors (VFs) enrichment comparison was conducted using mate analysis between the two groups, and P-values < 0.05 were considered significantly differential on gene expression. The differential abundance analysis, generation of the PCoA plots, box plots, heatmap and stacked bar charts were produced in R (version 3.2.0, https://www.r-project.org/) with appropriate statistical tests [15]. P-value < 0.05 was considered statistically significant.

Fig. 1. The clinical manifestation of SDRIFE-like skin toxicities of patient 1 by EGFR-TKI.
The manifestation of SDRIFE-like lesions at the anterior neck (A), axilla region (B) and popliteal fossa (C) when her admission.

3. Results

3.1. Treatment of the patient

Patient 1 was a 56-year-old Chinese woman who was diagnosed with pulmonary adenocarcinoma of right-middle lobe in 2016. She underwent surgery, during which no lymph node metastasis was found (0/26). Exon 21 of EGFR showed a mutation (L861Q). The bone and brain metastases were found in 2017 and 2018, respectively. Targeted therapy with afatinib was initiated but resulted in generalized pruritic erythematous lesions, particularly in flexural regions. Afatinib treatment was discontinued, and she was pre-scribed systemic corticosteroids (prednisone, 15 mg/d) and topical mometasone furoate cream, resulting in mild improvement. Despite this, she expressed a preference to restart afatinib, leading to the recurrence and worsening of the lesions, significantly impacting her quality of life.

On physical examination, the patient presented with SDRIFE-like lesions: well-demarcated erythema with exudation and crusting on flexural regions, including the anterior neck, axilla region, inframammary fold, antecubital fossae, femoral triangle, popliteal fossa, and periumbilical region (Fig. 1A–C, Supplementary Fig. 2A). The laboratory results were unremarkable (Supplementary Table 1). Subsequently, the patient was prescribed systemic corticosteroids (equivalent to prednisone 15–25 mg/d for 8 days) and wet wraps of the lesions with 3 % boric acid solution for 4 days until the exudation decreased. After five days, when the inflammation had reduced, minocycline (100 mg/d) was initiated, leading to significant improvement of her SDRIFE-like lesions observed three days later (Supplementary Fig. 2A) before her discharge. Oral corticosteroids were gradually tapered and discontinued within one week, while minocycline was taken intermittently. During the follow-up two months later, her SDRIFE-like lesions demonstrated sustained long-term improvement, except for those on the popliteal fossa (Supplementary Fig. 2B), which showed further improvement in the sub-sequent half-year follow-up (Supplementary Fig. 2C). She has not discontinued afatinib or reduced the dosage.

Patient 2 was a 53-year-old Chinese woman who was diagnosed with a pulmonary adenocarcinoma of right-lower lobe in 2019. She underwent surgery, during which lymph node metastasis was found (22/24). No mutations were detected in the EGFR exons. In August 2022, targeted therapy with dacomitinib, another second-generation EGFR-TKI, was initiated at a dose of 30 mg/d. One month prior to the visit, she developed generalized painful maculopapular lesions that significantly impacted her daily life. On physical examination, well-demarcated erythema and papula with exudation and crusting were observed, particularly on the buttocks, scalp/neck, and face (Fig. 2A–C). The laboratory results were unremarkable except for mildly elevated total white blood cell count and neutrophils. Notably, rapid improvement of her maculopapular lesions was observed after 7 days of minocycline treatment (100 mg/d, Supplementary Fig. 3B). Her original dose of dacomitinib was continued.

3.2. Decreased microbial diversity in the patient

Given the intra-group characteristics of bacterial composition among these 7 sites (Fig. 3A-B, Supplementary Figs. 4–5), samples from these sites were pooled together to make one representative sample respectively. A total of 1063114 sequences were obtained from the samples. The mean sequence length was 448 bp. The results of community richness (ACE: p = 4.01E-09; Chao1: p = 3.49E-09) and diversity index (Shannon: p = 0.0032; Simpson: p = 0.0032) indicated that the diversity of bacterial species was significantly lower in affected skin compared to healthy skin (Supplementary Fig. 6A); PCoA revealed disparately separated microbial communities. In the cluster of patient group, the samples from different skin sites were closely grouped together but significantly separated from the control group (Supplementary Fig. 6B). The apparent separation estimated by the first principal coordinate between the clusters in the two groups showed higher significant differences between these two bacterial communities. Furthermore, a non-parametric statistical test of ANOSIM, demonstrated the inter-group differences were greater than the intra-group differences (R = 1, p = 0.002,
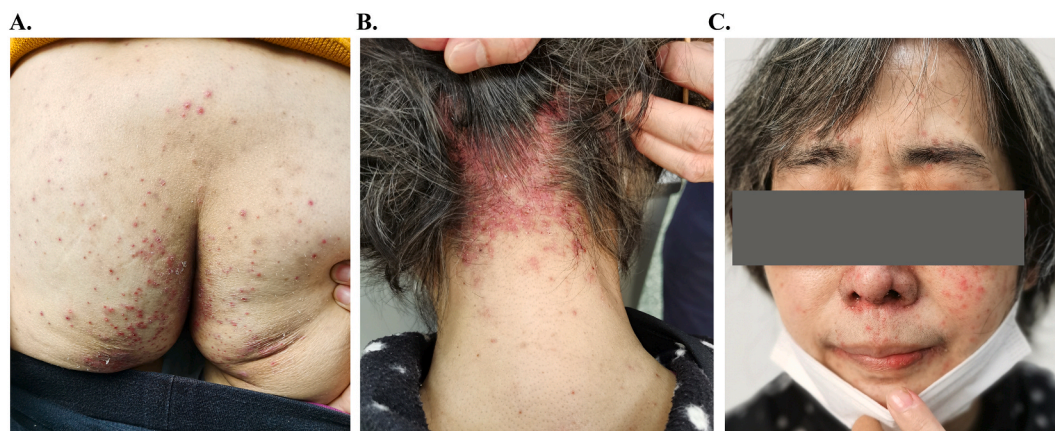

Fig. 2. The clinical manifestation of maculopapular toxicities of patient 2 by EGFR-TKI.
The manifestation of maculopapular lesions at the buttocks (A), scalp and neck (B), and her face (C) when her admission.
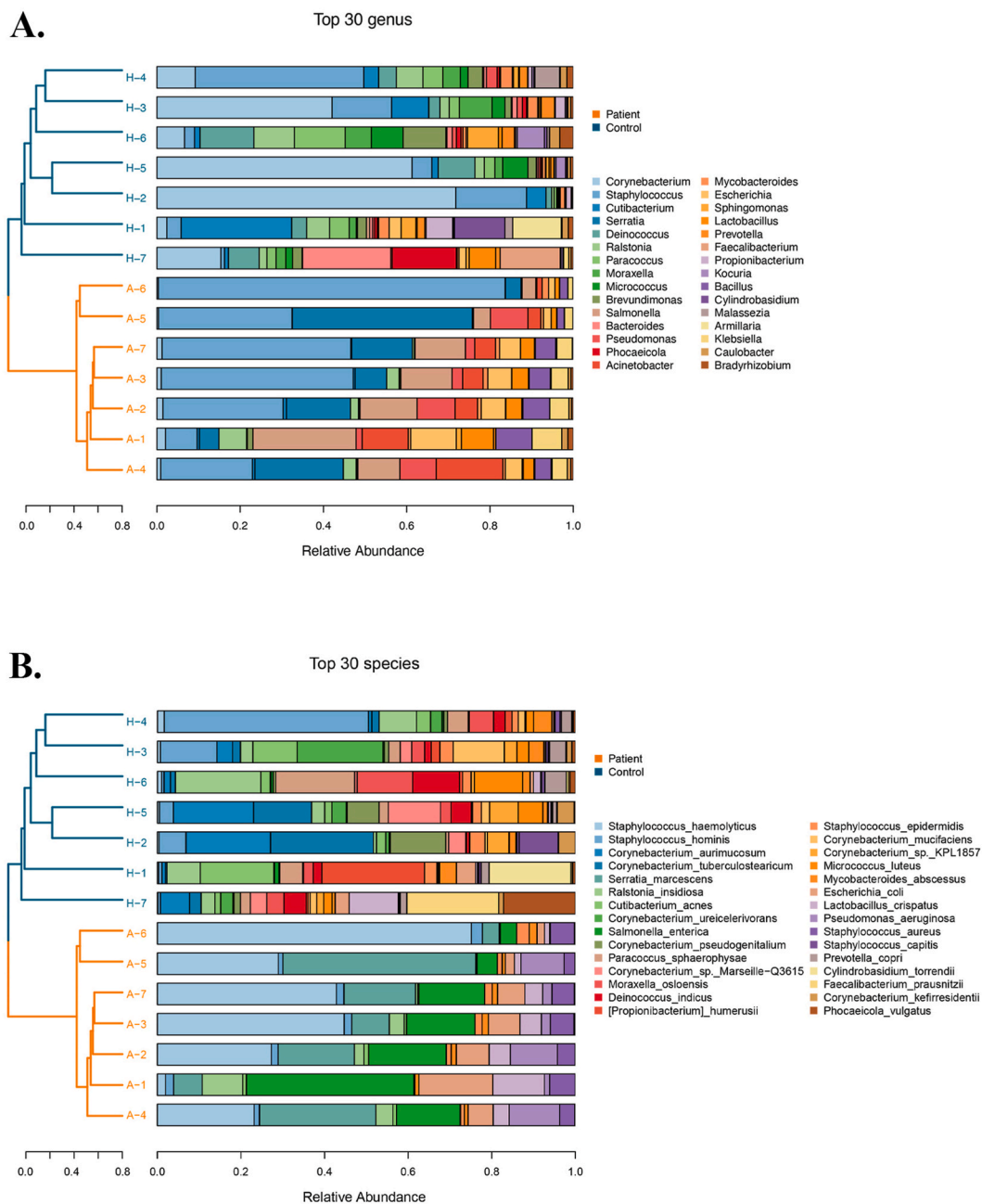
Fig. 3. The analysis graph combination of sample cluster tree and stacked bar chart.
On the left side is the hierarchical clustering analysis based on community composition (based on Bray Curtis distance algorithm) among samples, and on the right side is the bar chart of the top 30 microorganisms in relative abundance, representing the distribution of the basic community structure of the samples. Panel A is shown at the level of the genus and Panel B is shown at the species level.

Supplementary Fig. 6B). Overall, a significant decrease in microbial diversity was observed in the composition of bacterial communities in the patient group.

3.3. Altered microbial composition in lesions

The relative abundance patterns of all bacteria isolated from skin surface samples differed between healthy controls and subjects with skin toxicity. In addition to the changes at the genus level phylogenetically (Supplementary Fig. 6C), there were notable differences at the species level (Fig. 4). *Salmonella enterica, Escherichia coli, Staphylococcus haemolyticus, Staphylococcus aureus, Serratia*

marcescens and *Pseudomonas aeruginosa* had the highest relative abundance in affected lesions. Conversely, the abundance of skin commensals such as *Corynebacterium* sp*., Prevotella copri,* and *Staphylococcus epidermidis* was lower in patients after EGFR-TKI treatment compared to healthy controls.

3.4. Specific bacterial species differences between the patient and control group

The top 30 most abundant differential bacterial species were found to be less enriched in affected skin compared to healthy skin. Among these differentially abundant species, *S. haemolyticus* (p = 0.0111, FDR-adjusted p = 0.0294)*, S. aureus* (p = 0.0070, FDR-adjusted p = 0.0257)*, S. enterica* (p = 0.0006, FDR-adjusted p = 0.0093)*, Acinetobacter baumannii* (p = 0.0006, FDR-adjusted p = 0.0093)*, S. marcescens* (p = 0.0006, FDR-adjusted p = 0.0093) and *P. aeruginosa* (p = 0.0111, FDR-adjusted p = 0.0294) were the more notable species associated with affected skin microbiome. There was an extra *A. baumannii* and one missing species of *E. coli* compared to the six most abundant species in the affected skin in the above results (Supplementary Fig. 6D). These results essentially determined the dominant species that play key roles in the affected skin. There are also some species that are deficient in the affected skin. Furthermore, several species that were deficient in the affected skin were mostly consistent with the species mentioned earlier that were enriched in healthy controls, such as *S. epidermidis* (p = 0.0262, FDR-adjusted p = 0.0602), *P. humerusii* (p = 0.0021, FDR-adjusted p = 0.0142)*,* and several species of *Corynebacteriu*, which showed decreased abundance in the patient samples.

3.5. Microbiota-based module and bacterial species correlation in two groups

We explored the interactions of dominant species with other species. The species in Module 2 and Module 3 were closely related to each other, and most of them were in the healthy group. The dominant bacteria in patient group were mostly in modules 1, 4, and 5. Although *S. marcescens* (in Module 2), *S. enterica* (in Module 4) and *A. baumannii* (in Module 4) among the dominant species in the disease group had many associations with most members of Module 2 and Module 3, they were all negatively correlated. And positive
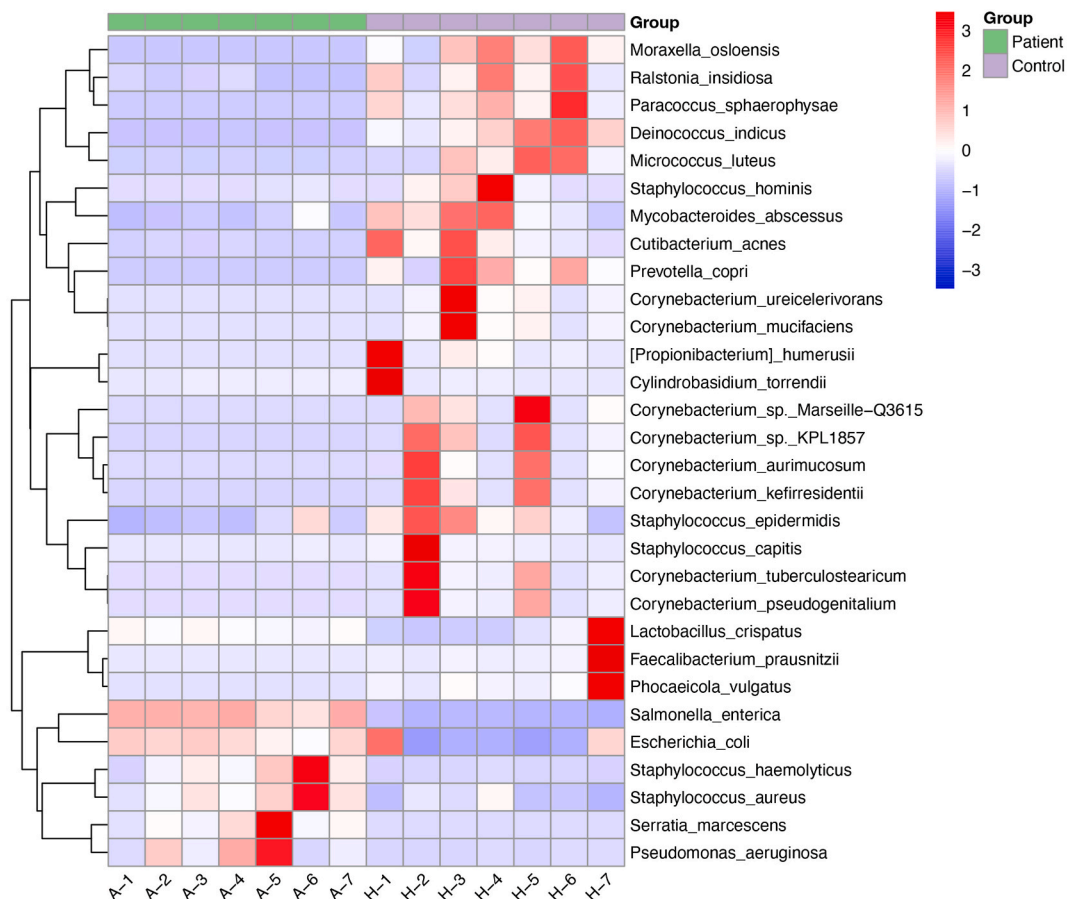

Fig. 4. Altered microbial composition in lesions.
The top 30 bacterial species ranked by abundance were selected, and their abundance information in each sample were used to build the heatmaps. Compositions of skin microbiomes at the species level in each skin sites were shown, summarized with average abundance. A: the patient; H: the controls.

correlations were shown with the other dominant pathogenic members (*S. haemolyticus*, *S. aureus* and *P. aeruginosa*) (Supplementary Fig. 7A). In the heatmap, the members of the seven dominant species mentioned above showed correlations with each other as expected (Supplementary Fig. 7B). Two members of the genus Staphylococcus, *S. aureus* and *S. haemolyticus* showed a close correlation with each other ($p < 0.001$). *E. coli* showed a positive correlation with *S. enterica* and *A. baumannii* ($p < 0.05$). *S. enterica, A. baumannii,*
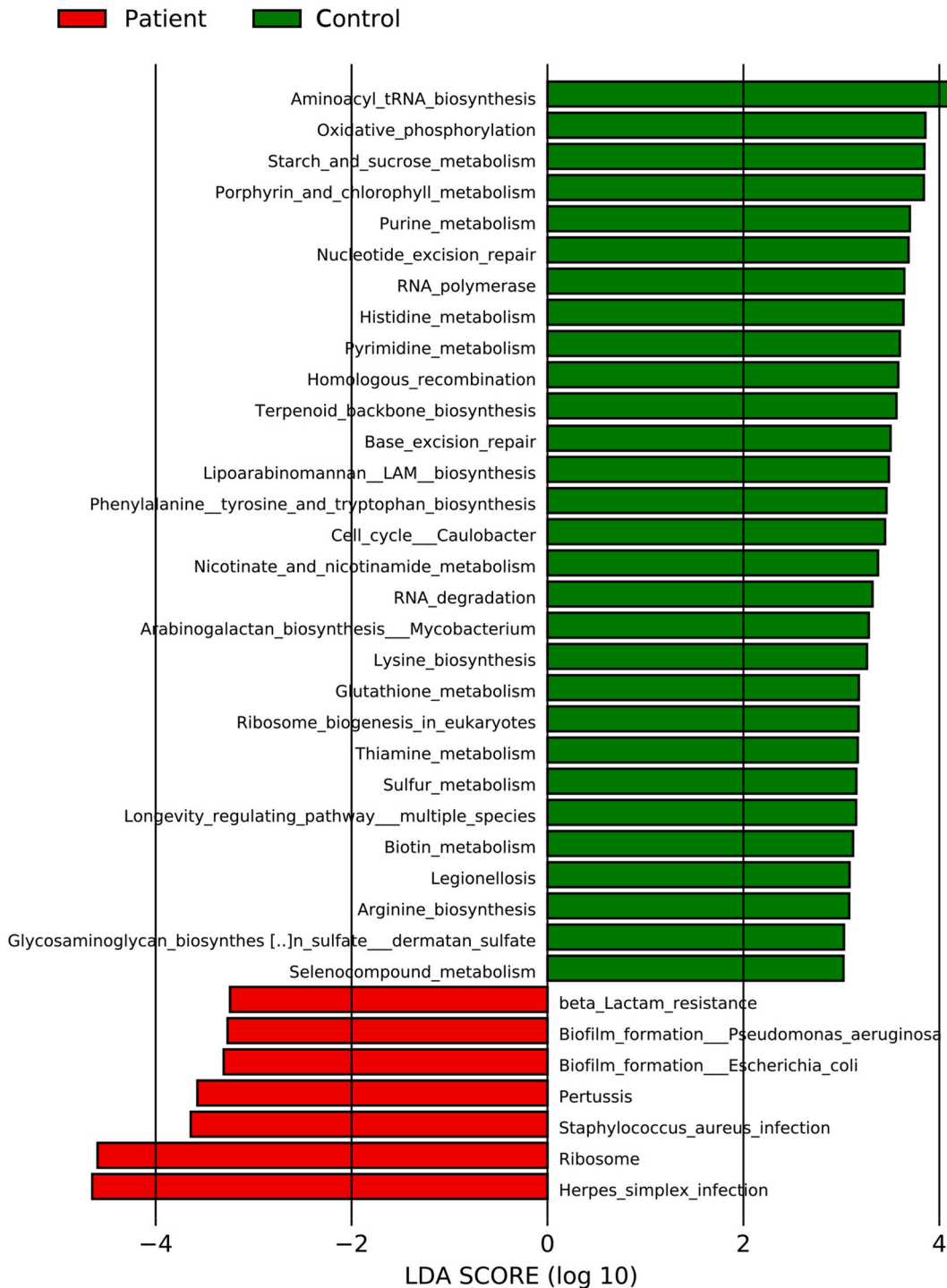

Fig. 5. Analysis of linear discriminant analysis (LDA) effect size (LEfSe).
To analyze the potential function profiles of the skin microbiota in the patient, we explored the distribution diagram of the LDA scores in two groups and results of the LEfSe analysis based on the LDA scores to screen the pathways of KEGG ($P < 0.05$ and LDA score/effect-size threshold = 3).

S. marcescens and *P. aeruginosa* were found positively correlated with each other (p < 0.01). Additionally, they were negatively correlated with some members of the healthy skin commensal microorganisms (Supplementary Fig. 7B).

3.6. Multi-dimensional functional changes by microbial dysbiosis in lesions

To explore potential differences in functions between the two groups, we aligned the metagenomic data with the third level of KEGG pathways and annotated a total of 105 pathways (Fig. 5). In the LEfSe analysis, we used the LDA value to estimate the effect size of each pathway on the differential effect. Based on the LDA scores, we identified 7 signature functional pathways in the skin disease group, including beta-Lactam resistance, Biofilm formation, and Staphylococcus aureus infection. Conversely, the results revealed that the skin surfaces of healthy controls were enriched with KEGG pathways associated with physiological benefits to skin symbiotic bacteria and skin: (1) key amino acid metabolism (tryptophan biosynthesis, histidine metabolism, glutathione metabolism); (2) energy metabolism (oxidative phosphorylation, sucrose and starch metabolism); (3) metabolism of cofactors and vitamins (thiamine, nicotinate and nicotinamide); (4) glycan biosynthesis (glycosaminoglycan, lipoarabinomannan, arabinogalactan) (Fig. 5).

To clarify whether VFs play a role in bacteria population dynamics during colonization, we annotated the metagenomic data against the virulence factor database (VFDB). As shown in Supplementary Fig. 8, there was no observed increase in microbial virulence for the lesions compared to the control group.

4. Discussion

The adverse effects of EGFR-TKIs on the skin are a serious concern and are of particular clinical interest, especially the toxicity resulting from on-target effects on wild-type EGFR (e.g., afatinib) [5,16–19]. Prophylaxis with minocycline has been recommended in decreasing the severity of the skin toxicity during EGFR-TKI treatment [20–22]. An analysis reported that prophylactic antibiotics may reduce the relative risk of severe rashes associated with EGFR-targeted agents by 42–77 % [23]. This suggests that microbial infection may play an important role in the skin adverse reactions induced by EGFR-TKIs.

The skin microbiome is known to play major roles in immune interactions, barrier repair, colonization resistance, and wound healing. Multiple studies have reported that the dysbiosis of the skin microbiome is associated with the onset and/or progression of many skin diseases, including atopic dermatitis, acne and psoriasis [24–26].

In our study, the patient developed SDRIFE-like dermatitis after taking afatinib. SDRIFE has been considered as a T-cell mediated hypersensitivity drug reaction, however, its exact pathogenesis remains unclear [27–29]. Common medications known to cause SDRIFE include aminopenicillins, β-lactam antibacterials, and targeted tumour therapy agents (e.g., EGFR inhibitor of gefitinib) [7]. To the best of our knowledge, this is the first published case of afatinib-induced SDRIFE-like lesions. The symmetrical erythematous manifestations and flexural regions involved suggest that microbial dysbiosis on the basis of skin barrier abnormalities may have occurred. Therefore, exploring skin microbiota composition and functionalities by metagenomic methods presents a promising strategy to gain insight into the SDRIFE-like toxicity caused by EGFR-TKI.

We initially observed a decrease in the diversity/richness of the lesional microbiota. Previous studies have reported significant reductions in microbiome diversity in conditions such as atopic dermatitis, seborrhoeic dermatitis, and psoriasis [30,31]. The diversity of the skin microbiota plays a crucial role in maintaining a robust immune-protective environment [32]. It has been demonstrated that individuals with low diversity and richness of gut bacteria exhibit more marked insulin resistance and a more pronounced inflammatory phenotype [33,34]. This suggests that decreased diversity/richness of lesional microbiota may be involved in flexural skin damage by afatinib. Nevertheless, conclusive evidence is needed to investigate whether a causal relationship exists in the skin in this manner. In addition to the observed low diversity/richness, the skin microbiota in patient group exhibited alterations, including increased proportions of pathogenic bacteria associated with atopic dermatitis, especially *S. aureus*. Conversely, the abundance of commensal skin bacteria decreased, including *S. epidermidis* and *C. acnes* (original name is *Propionibacterium acnes*). These commensal skin bacteria play a beneficial role in the human body. For instance, *S. epidermidis* produces antimicrobial peptides (AMPs) that work synergistically with AMPs derived from human epithelial cells to combat *S. aureus* [35]. The cell wall component of *S. epidermidis* mitigates inflammation by binding to toll-like receptor 2 (TLR2) on human keratinocyte, thereby limiting tissue damage and promoting skin barrier healing [25,36]. The observed changes in bacterial community composition indicate a role of microbial dysbiosis in the transition from healthy skin to affected skin by afatinib.

In addition to the observed decrease in microbial diversity/richness and alterations in composition, the LEfSe analysis revealed distinctive characteristics of several functional pathways that exhibited differences between the two groups. Firstly, the patient group displayed a distinct abundance of pathogenic bacterial infection (specifically *S. aureus* infection) and strong pathogenicity, as indicated by enhanced biofilm formation. Biofilm serves to facilitate bacterial attachment to surfaces and offers protection against host immune responses, antibiotics, and harsh environmental conditions [37]. Moreover, biofilm can impair the tissue repair processes and promote low-grade inflammatory persistence [38].

Secondly, the healthy control group exhibited an enrichment in pathways associated with factors beneficial to commensal bacteria on the skin and the physiology of the skin. In detail, these factors can be roughly divided into the following categories: (1) key amino acid metabolism (e.g., tryptophan biosynthesis); (2) energy metabolism (oxidative phosphorylation, sucrose/starch metabolism); (3) metabolism of cofactors and vitamins (thiamine, nicotinate and nicotinamide); (4) glycan biosynthesis (glycosaminoglycan, lipoarabinomannan, arabinogalactan).

Tryptophan is an essential amino acid and has been proposed as a therapeutic option for depression and stress [39]. The tryptophan metabolic pathway has been demonstrated to be attenuated in the skin microbiota of atopic dermatitis (AD) patients. The metabolite

indole-3-aldehyde (IAId) was found to be significantly reduced in both lesional and non-lesional skin of AD. IAId was proven to significantly attenuate skin inflammation in mouse AD-like dermatitis and regulate the expression of thymic stromal lymphopoietin (TSLP) in keratinocytes [40]. Our results showed that the tryptophan biosynthesis pathway in the skin microbiome of patients differed from that of the healthy group, which may be one of the important mechanisms of EGFR-TKI-induced skin damage.

We also observed a difference in the energy metabolism patterns of bacteria between the patient group and the healthy group. Specifically, we noted reductions in oxidative phosphorylation and sucrose/starch metabolism. The altered energy metabolic patterns probably participated in the skin damage by afatinib.

The functional pathways of the skin barrier were different between the adverse reaction group and healthy controls. It is known that lipid biosynthesis and glycan biosynthesis were significantly associated with cutis tissue development and wound healing. Glycosaminoglycans (GAGs) include dermatan sulphates (DS). Dermatan sulphate proteoglycans (DS-PGs) are widely distributed throughout the skin and possess potent biological activities that can regulate keratinocyte proliferation and differentiation, inflammatory processes, and the composition and quality of the extracellular matrix. This suggests that DS-PGs play a crucial role in the regulation of skin physiology [41,42]. Lipoarabinomannans (LAMs) are ligands for host glycan receptors such as TLRs and C-type lectin receptors on skin keratinocytes. The binding of LAMs to their receptors can train the skin immunity and skin barrier integrity [36]. Thus, from a physical barrier perspective, alterations in glycan biosynthesis may cause severe dysfunction in skin tissue repair and disruption of the skin barrier, ultimately facilitating the persistence of pathogenic bacteria.

It is noteworthy that the phenomena and characteristics mentioned above may play a crucial role in exacerbating adverse effects or alternatively, function as accompanying or subordinate factors. The determination of the conclusion requires further experimental research.

There are several limitations in this study. First, there is insufficient data on the dynamics of the skin microbiome during follow-up, as well as lack a comparison of bacterial flora after clinical healing of skin lesions. Next, the study sample size was relatively small and requires further validation through larger cohort studies and additional validation in independent cohorts and experimental models. Additionally, there are possible confounding factors, such as other medications or medical conditions that may also influence the composition of the cutaneous microbiome. Finally, the study focused on a specific group of patients with SDRIFE-like lesions induced by EGFR-TKI treatment. Therefore, the findings may not be directly applicable to other skin conditions or patient populations.

Taken together, our study provides primary data on the skin microbial dysbiosis and potential characteristics of SDRIFE-like AEs caused by EGFR-TKIs. With the wide application of small molecule inhibitors in targeting EGFR-driven cancer therapy, understanding the causes and characteristics of skin adverse reactions is especially important for their therapeutics. Our data support that microbial dysbiosis is involved in the occurrence of SDRIFE-like damage induced by EGFR-TKIs. Our findings also provide evidence for the application of antibiotics during the treatment of EGFR-TKIs and are beneficial for the adherence to anti-cancer therapy.

Data availability

The datasets generated during and/or analyzed during the current study are available from the corresponding author on reasonable request.

CRediT authorship contribution statement

Wenqi Liu: Conceptualization, Data curation, Investigation, Visualization, Writing – original draft. **Lu Peng:** Conceptualization, Data curation, Methodology, Visualization. **Ling Chen:** Investigation, Supervision, Writing – review & editing, Data curation. **Jianji Wan:** Conceptualization, Data curation, Project administration. **Shuang Lou:** Conceptualization, Data curation, Project administration, Writing – review & editing. **Tingting Yang:** Conceptualization, Data curation, Project administration. **Zhu Shen:** Conceptualization, Data curation, Funding acquisition, Methodology, Supervision, Writing – review & editing.

Declaration of competing interest

The authors declare that they have no known competing financial interests or personal relationships that could have appeared to influence the work reported in this paper.

Acknowledgement

Appendix A. Supplementary data

Supplementary data to this article can be found online at https://doi.org/10.1016/j.heliyon.2023.e21690.

IRB approval status: Reviewed and approved by the Ethics Committee of Guangdong People's Hospital IRB; approval # KY-N-022-109-01.

Patient Consent on File: Consent for the publication of recognizable patient photographs or other identifiable material was obtained by the authors and included at the time of article submission to the journal stating that all patients gave consent with the understanding that this information may be publicly available.

Reprint requests: Dr. Zhu Shen.

References

[1] P.L. Bedard, D.M. Hyman, M.S. Davids, et al., Small molecules, big impact: 20 years of targeted therapy in oncology, Lancet 395 (10229) (2020) 1078–1088.
[2] M.J. Ahn, J.M. Sun, S.H. Lee, et al., EGFR TKI combination with immunotherapy in non-small cell lung cancer, Expet Opin. Drug Saf. 16 (4) (2017) 465–469.
[3] S. Sigismund, D. Avanzato, L. Lanzetti, Emerging functions of the EGFR in cancer, Mol. Oncol. 12 (1) (2018) 3–20.
[4] E. Levantini, G. Maroni, M. Del Re, et al., EGFR signaling pathway as therapeutic target in human cancers, Semin. Cancer Biol. 85 (2022) 253–275.
[5] R.R. Shah, D.R. Shah, Safety and Tolerability of epidermal growth factor receptor (EGFR) tyrosine kinase inhibitors in oncology, Drug Saf. 42 (2) (2019) 181–198.
[6] A.S. Paller, H.H. Kong, P. Seed, et al., The microbiome in patients with atopic dermatitis, J. Allergy Clin. Immunol. 143 (1) (2019) 26–35.
[7] B. Copps, J.P. Lacroix, D. Sasseville, Symmetrical drug-related intertriginous and flexural exanthema secondary to epidermal growth factor receptor inhibitor gefitinib, JAAD Case Rep 6 (3) (2020) 172–175.
[8] W. Lewis, A. Forrestel, E. Baumrin, Epidermal growth factor receptor inhibitor-induced symmetrical drug-related intertriginous and flexural exanthema: should you discontinue the offending agent? Cutis 111 (1) (2023) 18–21.
[9] H. Wang, H.H. Chan, M.Y. Ni, et al., Bacteriophage of the skin microbiome in patients with psoriasis and healthy family controls, J. Invest. Dermatol. 140 (1) (2020), 182-90.e5.
[10] Z. Li, X. Bai, T. Peng, et al., New insights into the skin microbial communities and skin aging, Front. Microbiol. 11 (2020), 565549.
[11] P. Chitale, A.D. Lemenze, E.C. Fogarty, et al., A comprehensive update to the Mycobacterium tuberculosis H37Rv reference genome, Nat. Commun. 13 (1) (2022) 7068.
[12] Z. Ren, W. Luo, Metagenomic analysis reveals the diversity and distribution of antibiotic resistance genes in thermokarst lakes of the Yellow River Source Area, Environ Pollut 313 (2022), 120102.
[13] S. Chen, Y. Zhou, Y. Chen, et al., fastp: an ultra-fast all-in-one FASTQ preprocessor, Bioinformatics 34 (17) (2018) i884–i890.
[14] P. Ye, Y. Liu, Y.J. Cai, et al., Microbial community alteration in tongue squamous cell carcinoma, Appl. Microbiol. Biotechnol. 105 (21–22) (2021) 8457–8467.
[15] K.C. Tham, R. Lefferdink, K. Duan, et al., Distinct skin microbiome community structures in congenital ichthyosis, Br. J. Dermatol. 187 (4) (2022) 557–570.
[16] L.C. Tseng, K.H. Chen, C.L. Wang, et al., Effects of tyrosine kinase inhibitor therapy on skin toxicity and skin-related quality of life in patients with lung cancer: an observational study, Medicine (Baltim.) 99 (23) (2020), e20510.
[17] Y. Zhao, B. Cheng, Z. Chen, et al., Toxicity profile of epidermal growth factor receptor tyrosine kinase inhibitors for patients with lung cancer: a systematic review and network meta-analysis, Crit. Rev. Oncol. Hematol. 160 (2021), 103305.
[18] T. Yamaoka, S. Kusumoto, K. Ando, et al., Receptor tyrosine kinase-targeted cancer therapy, Int. J. Mol. Sci. 19 (11) (2018) 3491.
[19] Y. Honda, Y. Hattori, S. Katsura, et al., Stevens-Johnson syndrome-like erosive dermatitis possibly related to afatinib, Eur. J. Dermatol. 26 (4) (2016) 413–414.
[20] A. Scope, A.L. Agero, S.W. Dusza, et al., Randomized double-blind trial of prophylactic oral minocycline and topical tazarotene for cetuximab-associated acne-like eruption, J. Clin. Oncol. 25 (34) (2007) 5390–5396.
[21] K. Sano, K. Nakadate, K. Hanada, Minocycline prevents and repairs the skin disorder associated with afatinib, one of the epidermal growth factor receptor-tyrosine kinase inhibitors for non-small cell lung cancer, BMC Cancer 20 (1) (2020) 279.
[22] M. Yamada, H. Iihara, H. Fujii, et al., Prophylactic effect of oral minocycline in combination with topical steroid and skin care against panitumumab-induced acneiform rash in metastatic colorectal cancer patients, Anticancer Res. 35 (11) (2015) 6175–6181.
[23] J. Ocvirk, S. Heeger, P. McCloud, et al., A review of the treatment options for skin rash induced by EGFR-targeted therapies: evidence from randomized clinical trials and a meta-analysis, Radiol. Oncol. 47 (2) (2013) 166–175.
[24] B.K. Patel, K.H. Patel, R.Y. Huang, et al., The gut-skin microbiota Axis and its role in diabetic wound healing-A review based on current literature, Int. J. Mol. Sci. 23 (4) (2022) 2375.
[25] Y. Yang, L. Qu, I. Mijakovic, et al., Advances in the human skin microbiota and its roles in cutaneous diseases, Microb Cell Fact 21 (1) (2022) 176.
[26] P. Wan, J. Chen, A calm, dispassionate look at skin microbiota in atopic dermatitis: an integrative literature review, Dermatol. Ther. 10 (1) (2020) 53–61.
[27] S. Harbaoui, N. Litaiem, Symmetrical Drug-Related Intertriginous and Flexural Exanthema, StatPearls Publishing, Treasure Island (FL), 2022.
[28] M. Winnicki, N.H. Shear, A systematic approach to systemic contact dermatitis and symmetric drug-related intertriginous and flexural exanthema (SDRIFE): a closer look at these conditions and an approach to intertriginous eruptions, Am. J. Clin. Dermatol. 12 (3) (2011) 171–180.
[29] R. Ding, F.F. Cheo, H.Y. Lee, Celecoxib and bullous symmetrical drug-related intertriginous and flexural exanthem (SDRIFE), J. Allergy Clin. Immunol. Pract. 11 (2) (2023) 629–631.
[30] Y. Yu, S. Dunaway, J. Champer, et al., Changing our microbiome: probiotics in dermatology, Br. J. Dermatol. 182 (1) (2020) 39–46.
[31] I. Olejniczak-Staruch, M. Ciążyńska, D. Sobolewska-Sztychny, et al., Alterations of the skin and gut microbiome in psoriasis and psoriatic arthritis, Int. J. Mol. Sci. 22 (8) (2021) 3998.
[32] I. Ferček, L. Lugović-Mihić, A. Tambić-Andrašević, et al., Features of the skin microbiota in common inflammatory skin diseases, Life 11 (9) (2021) 962.
[33] S. Fang, R.M. Evans, Microbiology: wealth management in the gut, Nature 500 (7464) (2013) 538–539.
[34] E. Le Chatelier, T. Nielsen, J. Qin, et al., Richness of human gut microbiome correlates with metabolic markers, Nature 500 (7464) (2013) 541–546.
[35] A.M. Kemter, C.R. Nagler, Influences on allergic mechanisms through gut, lung, and skin microbiome exposures, J. Clin. Invest. 129 (4) (2019) 1483–1492.
[36] Y.E. Chen, M.A. Fischbach, Y. Belkaid, Skin microbiota-host interactions, Nature 553 (7689) (2018) 427–436.
[37] W. Yin, Y. Wang, L. Liu, et al., Biofilms: the microbial "protective clothing" in extreme environments, Int. J. Mol. Sci. 20 (14) (2019) 3423.
[38] Z. Versey, W.S. da Cruz Nizer, E. Russell, et al., Biofilm-innate immune interface: contribution to chronic wound formation, Front. Immunol. 12 (2021), 648554.
[39] A.S. Correia, N. Vale, Tryptophan metabolism in depression: a narrative review with a focus on serotonin and kynurenine pathways, Int. J. Mol. Sci. 23 (15) (2022) 8493.
[40] J. Yu, Y. Luo, Z. Zhu, et al., A tryptophan metabolite of the skin microbiota attenuates inflammation in patients with atopic dermatitis through the aryl hydrocarbon receptor, J. Allergy Clin. Immunol. 143 (6) (2019), 2108-19.e12.
[41] S.T. Wang, B.H. Neo, R.J. Betts, Glycosaminoglycans: sweet as sugar targets for topical skin anti-aging, Clin Cosmet Investig Dermatol 14 (2021) 1227–1246.
[42] S. Mizumoto, S. Yamada, The specific role of dermatan sulfate as an instructive glycosaminoglycan in tissue development, Int. J. Mol. Sci. 23 (13) (2022) 7485.